Instruments and Experimental Techniques, Vol. 41, No. 6, 1998, pp. 792–796. Translated from Pribory i Tekhnika Eksperimenta, No. 6, 1998, pp. 54–58.

NUCLEAR EXPERIMENTAL TECHNIQUES

Position Measurements of Electrons and γ-Quanta in the PHENIX Electromagnetic Calorimeter

A. V. Bazilevskii*, A. A. Durum*, E. P. Kistenev, V. I. Kochetkov*, V. K. Semenov*, and S. White****

* *Institute for High Energy Physics, Protvino, Moscow oblast, 142284 Russia*

** *Brookhaven National Laboratory, USA*

Received March 27, 1998

Abstract—Position resolution of the electromagnetic calorimeter for the PHENIX setup (RHIC, BNL) was studied at electron (photon) energies of 0.5–8 GeV and angles of incidence of 0°–20° with respect to the normal to the calorimeter surface. The features of the electron (photon) position reconstruction for nonorthogonal incidence are discussed.

INTRODUCTION

The PHENIX project aimed at the detection and study of quark–gluon-plasma properties is currently underway at the Brookhaven National Laboratory, USA [1]. Reliable identification of direct photons and measurement of their characteristics is one of the most powerful methods for identifying quark–gluon plasma and measuring its properties in the PHENIX experiment. For this purpose, a hodoscope lead–scintillator electromagnetic calorimeter with a total area of ~48 m^2 is under development. The calorimeter cell measures ~55 × 55 mm^2. The length of the calorimeter module is $18X_0$. A more detailed description of the PHENIX electromagnetic PbSc-calorimeter may be found in [2].

The calorimeter is designed to identify electrons and photons and measure their energy and positions of their points of incidence. The detector capability of detecting and measuring a signal from direct photons and of reconstructing π^0- and η-meson decays into γ-quanta pairs is directly connected with its energy and spatial resolution.

In this work, we present the measured position resolution of the PHENIX electromagnetic PbSc-calorimeter at electron (photon) energies of 0.5–8 GeV and angles of incidence of 0°–20° with respect to the normal to the calorimeter surface. The features of the electron (photon) position reconstruction for nonorthogonal incidence are discussed. The experimental data obtained during the sessions at the AGS accelerator (BNL, USA) and the results of the simulation using the GEANT package are presented.

POSITION MEASUREMENTS FOR ORTHOGONAL ELECTRON (PHOTON) INCIDENCE ON THE CALORIMETER

The simplest algorithm for determining positions of high-energy γ-quanta and electrons (positrons) in the cellular calorimeter is to measure the center of gravity of the shower X_{CG} [3]:

$$X_{CG} = \sum x_i w_i / \sum w_i, \quad w_i = E_i, \tag{1}$$

where x_i and E_i are the center position and the signal amplitude for the ith cell, respectively. Because of the finite cell width h and the pronounced shower attenuation within the cell limits, relationship (1) leads to the shifted position estimate [4]. The value of this shift depends on the position of the impact point on the cell. Using the single-exponential model for the cross shower profile [3], we can easily derive the following expression for the center of gravity of the shower (in terms of h):

$$X_{CG} = \frac{1}{2}\frac{\sinh(t/b)}{\sinh(1/2b)}, \quad |t| \le 1/2. \tag{2}$$

Here t is the position of the shower axis in the cell (t = 0 corresponds to the center of the cell) and b is the attenuation parameter in the single-exponential model of the cross shower profile (shower width). After the inverse transformation, we obtain the relationship for determining the shower-axis position in the cell [3]:

$$X_{\text{ash}} \equiv t = b\,\text{arcsh}(2X_{CG}\sinh(1/2b)), \quad |X_{CG}|) \le 1/2. \tag{3}$$

The origin of coordinates is placed at the center of the cell containing the center of gravity of the shower X_{CG}.

The particle position is estimated using the modified definition for the center of gravity of the shower [5]. It includes weights that are a nonlinear logarithmic function of energy:

$$X_{\log} = \sum x_i w_i^* / \sum w_i^*, \qquad w_i^* = \max\left(0, w_0 + \ln\frac{E_i}{\sum E_i}\right), \tag{4}$$

0020-4412/98/4106-0792$20.00

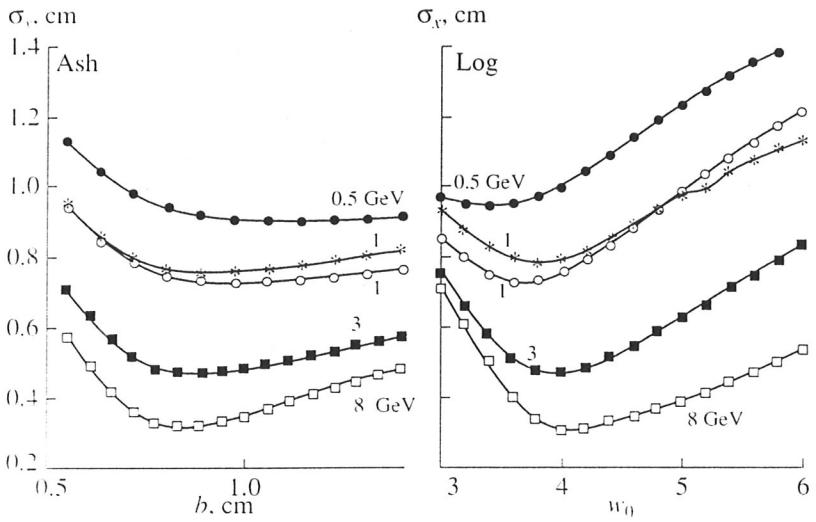

Fig. 1. The cell-average position resolution of the calorimeter as a function of parameters b in the method (3) and w_0 in the method (4). The experimental results at 1-GeV energy are marked with asterisks. The other curves are the results of the GEANT calculations.

where w_0 is the free parameter playing a double role. First, it sets a threshold for the fraction of the total shower energy deposited in the tower, because the channel could make its contribution to the calculation of the coordinate (4). Second, it controls the contribution of the shower periphery to the coordinate measurements.

The parameters b and w_0 in (3) and (4) may be found by minimizing the cell-average spatial resolution of the calorimeter σ_X. The dependence of σ_X on these parameters at various energies is shown in Fig. 1. The best resolution for (3) is achieved at a b value of ~8.5 mm, which is virtually independent of energy. The optimal value of w_0, at which the position resolution is at a minimum, increases from ~3.0 to ~4.0, with energy increasing from 0.5 to 8 GeV.

The value of parameter b may also be determined by fitting the experimental dependence $X_{CG}(t)$ with expression (2). The value $b \sim 8$ mm, determined from the fit, agrees well with the b value that corresponds to the σ_X minimum.

Formulas (3) and (4) give virtually the same average coordinate resolution over the calorimeter (Fig. 2), which is well parametrized by the expression

$$\sigma_X(E) = 1.55 + \frac{5.7}{\sqrt{E(\text{GeV})}} \text{ (mm)}. \qquad (5)$$

COORDINATE MEASUREMENTS FOR NONORTHOGONAL INCIDENCE

The spatial distribution of the energy release along the shower axis is symmetric about the axis and is shaped as a spindle with a gradually tapered tail, in which the energy release is small and undergoes strong fluctuations.

For orthogonal incidence of a particle on the calorimeter, the directions of the shower-symmetry axis and the normal coincide. Therefore, the shapes of the cross profile and projection of the shower onto the calorimeter plane coincide as well. The projection is shaped as a circle and is independent of the trend of the cascade curve.

In the case of oblique incidence, the directions of the shower axis and the normal fail to coincide, and the shape of the shower profile in the calorimeter plane is governed by the projection of the spindle-shaped figure onto this plane. It does not display axial symmetry and is shaped as a stretched ellipse with a larger axis

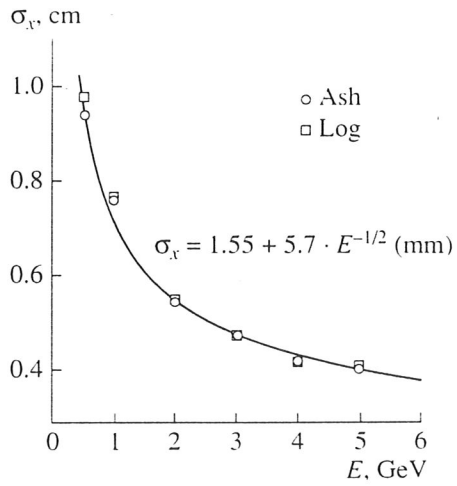

Fig. 2. The energy dependence of the cell-average position resolution of the calorimeter for orthogonal electron (photon) incidence in the Ash- and Log-methods described by (3) and (4), respectively (dots are the experimental results).

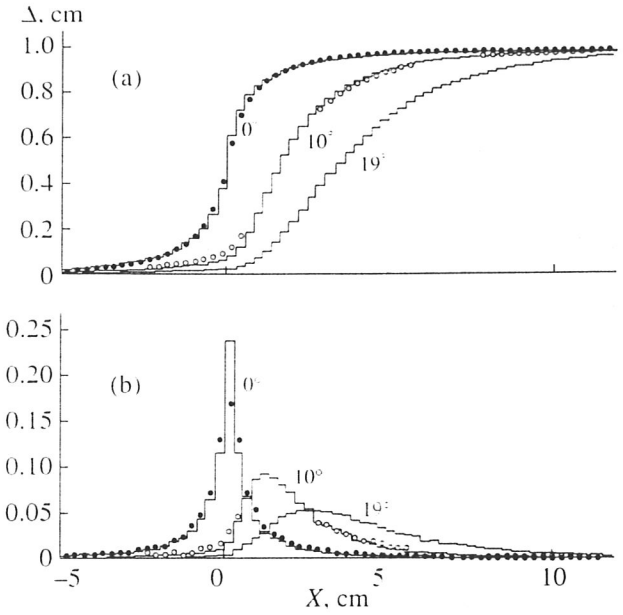

Fig. 3. (a) The integral and (b) differential one-dimensional distributions of the energy-release density of the shower along the X-axis (integration was performed along the Y-coordinate), for electrons with the 1-GeV energy, impact point $X = 0$, and inclination angles of 0°, 10°, and 19°. The data are obtained by simulation (histograms) and direct measurements on the beam (light and dark dots).

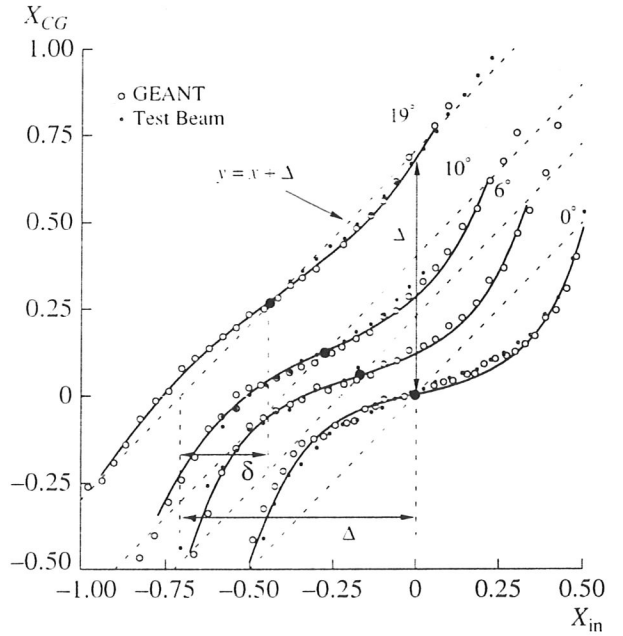

Fig. 4. The dependence of the center of gravity of the shower X_{CG} on the impact point X_{in} at incident angles of 0°, 6°, 10°, and 19°, for 1-GeV electrons. The fitted dependences (6) are shown with solid lines. The values of the parameters Δ and δ in (6) are presented for the curve with the angle of incidence equal to 19°. The point (0, 0) corresponds to the center of one of the towers. Dark dots are the experimental data and light dots are the simulation results.

directed along the projection of the particle-momentum vector onto the calorimeter plane.

The integral one-dimensional distributions of the energy deposited along the larger axis of the ellipse for a 1-GeV electron; the impact point $X = 0$; and the angles of incidence of 0°, 10°, and 19° are shown in Fig. 3a (the angle varies in the XZ plane, and the Z axis (normal) is directed along the axis of the calorimeter module). The appropriate differential distributions are shown in Fig. 3c. These data were obtained by both simulation (histograms) and direct measurements on the beam (light and dark dots). As is seen in Fig. 3b, the shower profile for the nonzero angle of incidence becomes asymmetric and is displaced from the particle impact point on the detector. The effective shower width along the X axis increases with the increasing angle.

It is characteristic that these distributions have long "tails" determined by the cascade-curve shape. The statistical fluctuations are very large here and may result in a systematic drift of the estimated impact-point position and in the deteriorated position resolution.

Using the energy release in the calorimeter cells, the position of the center of gravity X_{CG} was calculated for the varying coordinate of the impact point X_{in}. Thus obtained dependences $X_{CG}(X_{in})$ are presented in Fig. 4 for 1-GeV electrons and angles of inclination $\theta = 0°$, 6°, 10°, and 19°. The results of simulations and measurements are shown with light and dark dots, respectively. These data were approximated by the expression similar to (2).

The result of fitting is shown in Fig. 4 with solid lines. As is seen from the figure, the data are well described by (6) with three parameters characterizing the shower width b, displacement Δ of the calculated coordinate X_{CG} from the impact point X_{in}, and the phase of the $X_{CG}(X_{in})$-curve variations about the straight line $y = x + \Delta$.

The effective shower width increases with the angle, resulting in the decreasing amplitude of the $X_{CG}(X_{in})$-curve variations about the straight line $y = x + \Delta$. The shower-profile asymmetry at nonzero angles must lead to the distortion of the curve $X_{CG}(X_{in})$ obtained at 0°. This effect manifests itself most strongly in phase displacement of the curve variations $\delta \neq 0$.

$$X_{CG}(X_{in}) = \frac{1}{2}\frac{\sinh\left(\dfrac{X_{in} + \Delta - \delta}{b}\right)}{\sinh(1/2b)} + \delta; \qquad (6)$$

$$|X_{in} + \Delta - \delta| \leq \frac{1}{2}.$$

All of these parameters (b, Δ, and δ) depend on both the incident-particle energy and the angle of incidence. Analyzing the data from Fig. 4 at various energies and inclinations, it is possible to reveal the behavior of these functions. The results of this analysis are shown in Fig. 5.

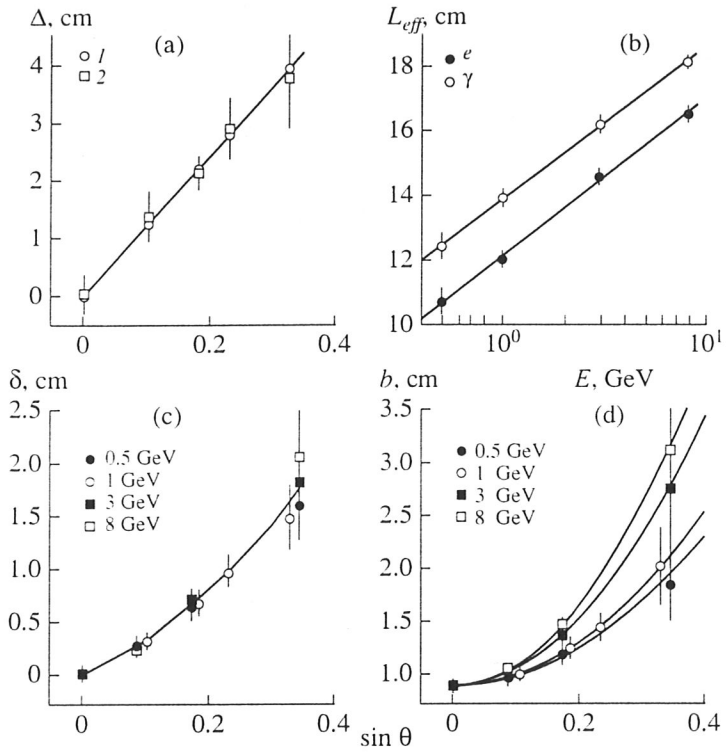

Fig. 5. (a) The dependence of Δ on sinθ for 1-GeV electrons: (*1*) simulation, (*2*) experiment, and the straight line is the result of fitting (7); (b) $L_{\text{eff}}(E)$ for photons and electrons; (c) δ(sinθ) and (d) b(sinθ) at various particle energies.

The angular dependence of the Δ-parameter is shown in Fig. 5a for 1-GeV electrons. The simulation results and the experimental data can be described by the linear function

$$\Delta = L_{\text{eff}} \sin\theta, \tag{7}$$

where L_{eff} is the effective depth of the shower penetration in the calorimeter, determined by the position of the cascade-curve median in the longitudinal direction.

The value of L_{eff}, calculated from (7), is presented in Fig. 5b as a function of the photon and electron energy.

As is shown in Fig. 5b, L_{eff} is a linear function of $\ln(E)$. Its value for photons exceeds L_{eff} for electrons by (1.8 ± 0.2) cm $= (0.9 \pm 0.1)X_0$ (where the radiation length in the calorimeter module is $X_0 \simeq 2$ cm). This agrees well with the behavior of the cascade-curve median (longitudinal profile of the electromagnetic-shower energy release) [6]. The value of the parameter δ is virtually energy-independent (Fig. 5c). The effective shower width b is shown in Fig. 5d as a function of the angle of incidence and the particle energy. In order to reconstruct the electromagnetic-shower coordinates, the data in Fig. 5d are approximated by the function quadratic in sin(θ).

The position of the particle impact on the calorimeter X_{in} was calculated according to the formula obtained by inverting (6):

$$X_{\text{ash}} = b\,\text{arcsh}[2(X_{CG} - \delta)\sinh(1/2b)] - \Delta + \delta, \quad |X_{CG} - \delta| \le \frac{1}{2}. \tag{8}$$

This method has permitted virtually complete compensation of the systematic error in measuring the electro-

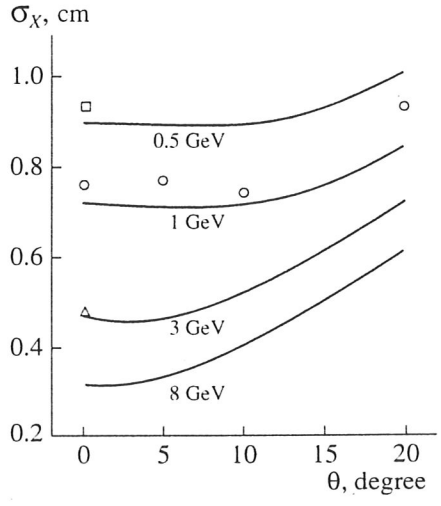

Fig. 6. The position resolution as a function of angle at electron energies of 0.5, 1, 3, and 8 GeV. The experimental results are shown with dots.

magnetic-shower coordinates in the incident-angle range of 0°–20°. The cell-average coordinate resolution of the detector is shown in Fig. 6 as a function of the angle at various shower energies. At small angles, the increasing effective shower energy leads to a slight improvement of σ_X. At large angles, the longitudinal shower fluctuations become predominant, which results in the deteriorating position resolution of the calorimeter. This effect manifests itself most strongly at energies from 3 GeV and on. In this case, the position resolution is well parametrized by the formula

$$\sigma_X(E, \theta) = \sigma_X(E, 0°) \oplus (d \sin(\theta)), \quad (9)$$

where $\sigma_X(E, 0°)$ is the position resolution for the orthogonal incidence {see (5)}. The second term in this expression describes the contribution of the longitudinal shower fluctuations. The value of the parameter d is about 1.6 cm, which corresponds to $0.8X_0$.

CONCLUSION

The position resolution of the electromagnetic lead–scintillator calorimeter of the PHENIX setup was investigated at angles of incidence from 0° to 20°. It was shown that, at nonzero angle of incidence of electron (photon) on the calorimeter, the electromagnetic-shower profile onto the detector plane became asymmetric and its center of gravity was displaced from the impact point of the particle. In this case, the effective shower width increased with increasing energy and angle. The cell-average displacement of the estimated center of gravity of the shower (1) could be represented as a displacement of the cascade-curve median in projection onto the calorimeter plane. The dependence of the calorimeter position resolution on the angle and the particle energy was studied.

In conclusion, the work is based on the analysis of the events simulated with the GEANT package. The experimental data at hand agree well with the simulation results.

ACKNOWLEDGMENTS

We are grateful to V.A. Bumazhnov for his help in the development of the program for simulating showers in the PbSc-calorimeter, V.A. Onuchin for useful discussions, and all the members of the PHENIX group, who took part in the AGS-accelerator sessions in 1995–1996, for their help in data acquisition and analysis.

REFERENCES

1. *PHENIX Conceptual Sesign Report*, 29 January, 1993.
2. David, G., Kistenev, E., Patwa, A., *et al.*, *IEEE Trans. Nucl. Sci.*, 1996, vol. 43, no. 3, p. 149.
3. Akopgjanov, G.A., Inyakin, A.V., Kachanov, V.A., *et al.*, *Nucl. Instrum. Methods Phys. Res.*, 1977, vol. 140, p. 441.
4. Barkov, B.P., Katinov, Yu.V., Semenov, V.K., *et al.*, *Prib. Tekh. Eksp.*, 1994, no. 3, p. 66.
5. Awes, T.C., Obenshain, F.E., Plasil, F., *et al.*, *Nucl. Instrum. Methods Phys. Res., Sect. A*, 1992, vol. 311, p. 130.
6. Rabin, N.V., *Prib. Tekh. Eksp.*, 1992, no. 1, p. 20.